In-plane thermal conductivity of large single crystals of Sm-substituted $(Y_{1-x}Sm_x)Ba_2Cu_3O_{7-\delta}$

M.Matsukawa,H.Noto and H.Furusawa

E-mail: matsukawa@iwate-u.ac.jp
Department of Materials Science and Technology, Iwate University , Morioka 020-8551 , Japan

X.Yao

Department of Physics, Shanhai Jiao Tong University, Shanghai 200030, People's Republic of China

S.Nimori

National Institute for Materials Science, Tsukuba 305-0047 ,Japan

N. Kobayashi

Institute for Materials Research, Tohoku University, Sendai 980-8577, Japan

Y.Shiohara

Superconducting Research Laboratory, ISTEC,Tokyo 135-0062, Japan

Abstract. We have investigated the in-plane thermal conductivity $\kappa_{ab}(T,H)$ of large single crystals of optimally oxygen-doped $(Y_{1-x},Sm_x)Ba_2Cu_3O_{7-\delta}$ (x=0, 0.1, 0.2 and 1.0) and $YBa_2(Cu_{1-y}Zn_y)_3O_{7-\delta}$(y=0.0071) as functions of temperature and magnetic field (along the c axis). For comparison, the temperature dependence of κ_{ab} for as-grown crystals with the corresponding compositions are presented. The nonlinear field dependence of κ_{ab} for all crystals was observed at relatively low fields near a half of T_c. We make fits of the $\kappa(H)$ data to an electron contribution model, providing both the mean free path of quasiparticles ℓ_0 and the electronic thermal conductivity κ_e, in the absence of field. The local lattice distortion due to the Sm substitution for Y suppresses both the phonon and electron contributions. On the other hand, the light Zn doping into the CuO_2 planes affects solely the electron component below T_c, resulting in a substantial decrease in ℓ_0 .

1. Introduction

Since the discovery of high-T_c cuprate with its perovskite structure, a large number of measurements of thermal conductivity κ have been reported up to date, giving crucial information about transport properties in the superconducting and normal states[1]. The thermal conductivity of solids is usually separated into the phonon and electronic components κ_{ph} and κ_e [2]. For high-T_c copper oxide superconductors $YBa_2Cu_3O_{7-\delta}$(YBCO), $Bi_2Sr_2CaCu_2O_{8+\delta}$ and $Tl_2Sr_2CaCu_2O_{8+\delta}$, a rapid enhancement in $\kappa(T)$ is observed below T_c, with decreasing T, then $\kappa(T)$ reaches a maximum around a half of T_c and finally shows a monotonous decrease at low temperatures. Tewordt et al. ascribed the origin of the anomaly to the phonon contribution κ_{ph} on the basis of the classical theory of thermal transport in superconductors [3]. On the contrary, Yu et al. have proposed a new interpretation of the anomalous enhancement in $\kappa(T)$ as being responsible for the electron contribution κ_e [4]. Following their proposal, a strong suppression in the quasiparticle scattering rate below T_c causes the $\kappa(T)$ anomaly, which is consistent with an observed peak in measurements of microwave conductivity in $YBa_2Cu_3O_{7-\delta}$ [5]. In addition, the magnetic field effect on the thermal conductivity in high-T_c superconductors enables us to examine the scattering processes of thermal carriers due to magnetic vortex lines [6, 7]. In ref. [8], the authors developed a two component method to analyze the field dependence of the thermal conductivity and concluded that only the electronic contribution is field sensitive. In a similar way, a procedure to check the linear field dependence of inverse electronic thermal conductivity was proposed by Pogorelov et al. [9]. However, the origin of the anomalous peak in $\kappa(T)$ and its field dependence are still open questions.

In this paper, we present measurements of the in-plane thermal conductivity κ_{ab} of Sm-substituted single crystals $(Y_{1-x},Sm_x)Ba_2Cu_3O_{7-\delta}$ (x=0, 0.1, 0.2 and 1.0) as functions of temperature and magnetic field. To our knowledge, no measurement of thermal conductivity has been performed on A-site substituted single crystals YBCO except for polycrystalline samples [10, 11]. Here, we give some comments on the substitution effect of Sm ion on the crystal growth of $YBa_2Cu_3O_{7-\delta}$. In a previous work, the substitution of Sm for Y led to a high growth rate for single crystal growth, which is about two times greater with a Sm content x=0.12 than that of YBCO [12]. Moreover, by controlling the Sm content, one obtained high superconductivity for Sm substituted YBCO.

The $\kappa(H)$ profile is fitted using the electron contribution model, to estimate the mean free path of quasi particles ℓ_0 near a half of T_c in the absence of field [8, 13]. Compared with the linear field dependence of the inverse κ_e ,the square-root fit to the $\kappa(H)$data is applied . In addition, we discuss the impurity substitution effect on the thermal conduction of large single crystals $YBa_2Cu_3O_{7-\delta}$.

2. Experiment

A series of single crystalline $(Y_{1-x},Sm_x)Ba_2Cu_3O_{7-\delta}$ (x=0, 0.1, 0.2 and 1.0) and $YBa_2(Cu_{1-y}Zn_y)_3O_{7-\delta}$ (y=0.0071) were grown by the crystal pulling method. Sm contents range from 0, 0.1(0.119),0.2(0.215) and 1.0. As-grown crystals with x=0, 0.1, 0.2 and y(Zn)=0.0071 were annealed at 520°C in the oxygen atmosphere (for 1 to 2 weeks)to achieve the optimal T_c with $7-\delta =\sim 6.9$, as shown in Fig.2. $SmBa_2Cu_3O_{7-\delta}$ (SmBCO) crystal was oxidized at 300°C for 200h, giving a higher T_c property. The slight degradation in T_c for SmBCO probably arises from the partial substitution of Sm for Ba site rather than oxygen defects because we annealed it in the oxygen atmosphere for a very long time. The oxygen content for the as-grown crystal with x=0 was estimated to be $7-\delta =\sim 6.17$ using the iodometric analysis on one piece cut from the same batch. Sample preparations are described by Yao et al.in [12, 14, 15]. Sample dimensions are typically 4.5×3.1 mm^2 in the *ab*-plane and 1.7 mm along the *c*-axis. The EPMA analysis showed that Sm ion is uniformly distributed in single crystals. The inductively coupled plasma (ICP) technique revealed that single crystalline samples used in our measurements are close to the nominal compositions.

Measurements of the thermal conductivity, in the *ab*-plane and along the *c*-axis, were done with a conventional steady-state heat-flow method[16]. The magnetic field effect on the *ab*-plane thermal conductivity was examined in the application of fields up to 14 T along the *c*-axis at the Tsukuba Magnet Laboratory, the National Institute for Materials Science and at the High Field Laboratory for Superconducting Materials, Institute for Materials Research, Tohoku University. A temperature gradient across the sample was determined using a differential-type Chromel-constantan thermocouple after a calibration procedure. The magnetization measurement was carried out using the SQUID magnetometer. The temperature variation of the resistivity was measured on the identical samples using a four-probe technique.

3. Results and discussion

The in-plane thermal conductivity κ_{ab} for single crystals $(Y_{1-x},Sm_x)Ba_2Cu_3O_{7-\delta}$ (x=0, 0.1, 0.2 and 1.0) and $YBa_2(Cu_{1-y}Zn_y)_3O_{7-\delta}$ (y=0.0071) is shown as a function of temperature in Fig.1. For comparison, the out-of-plane thermal conductivity $\kappa_c$with x=0 and 1.0 is also depicted in the Fig.1. For the identical crystals used for our experiment , measurements of the low-field magnetization and the in-plane resistivity are presented in Fig.2, to check the superconducting properties. The resistivity data for the lightly Zn doped sample will be shown in the inset of Fig.3(b).

First of all, the κ_{ab} of $(Y_{1-x},Sm_x)Ba_2Cu_3O_{7-\delta}$ showed a rapid enhancement upon crossing T_c with decreasing temperature, while for κ_c no remarkable variation was detected near T_c. The substitution of Y by Sm strongly suppresses a maximum of κ_{ab} from 160 mW/cmK at x=0 down to 50 mW/cmK at x=0.2 through 85 mW/cmK at x=0.1. However, the pronounced peak of κ_{ab} below T_c is still observed even for the

x=0.2 crystal with its low thermal value. For the SmBCO crystal, κ_{ab} exhibits a low thermal conductivity accompanied by the broad maximum near 40K. This finding is closely related to a local lattice distortion due to the slight substitution of Sm for Ba as mentioned before. For free ions, the effective moment of Sm^{3+} is 0.85 μ_B and it is much smaller than the value of other rare earth ions (3.62 μ_B for Nd^{3+} and 7.96 μ_B for Gd^{3+}). If the phonon scattering due to magnetic ions with the smaller moment is assumed to be in the presence of the crystal field for SmBCO, it will contribute a suppression observed in κ_{ab} to some extent.

Now, we comment on κ in the normal state for the superconducting crystals. The thermal conductivity is separated into the electronic and phonon components. First, the electronic thermal conductivity in the normal state κ_e^n is estimated from the resistivity data using the Wiedemann-Franz (WF) law $\kappa_e^n = L_0T/\rho$ with a Lorentz number L_0 =2.45×10^{-8}WΩ/K^2. For all superconducting crystals, the estimated value κ_e^n is almost independent of T because of the T linear dependence of ρ, as shown in Fig.3(a). Accordingly, when $\kappa_{ab} - \kappa_e^n$ gives rise to the phonon component $\kappa_{ph}(T)$, the T dependence of $\kappa_{ab}(T)$ observed represents that of the phonon component in the normal state [17].

For comparison, let us show in Fig.3(b) the κ_{ab} data for the corresponding as-grown crystals of $(Y_{1-x},Sm_x)Ba_2Cu_3O_{7-\delta}$ (x=0 and 0.1) and $YBa_2(Cu_{1-y}Zn_y)_3O_{7-\delta}$ (y=0.0071) . In the inset of Fig.3(b), the as-grown ρ data for the Zn-doped sample are presented and the electronic component κ_e^n is neglected from the WF law using its resistivity data. For other as-grown crystals, we also expect an insulating property or a weakly metallic one with high resistivity. We note that the as-grown crystals for our experiment were prepared at least under the similar crystal growth environment. Accordingly, we conclude that for all as-grown crystals used, $\kappa \approx \kappa_{ph}$.

The κ_{ab} at x=0 follows a weakly T^{-1}-like behavior, while for the Sm - substituted crystal it is almost independent on T. This finding is probably caused by the enhanced phonon scattering due to the Sm substitution. Here, At high temperatures, the T dependence of $\kappa_{ab}(T)$ of the as-grown crystal is expressed as $\kappa_{ph} = 1/(W_0 + \alpha T)$, where W_0 and α are thermal resistances due to defect scattering and phonon-phonon Umklapp scattering, respectively. Moreover, for the light Zn doping for the as-grown sample we observed a similar T dependence of κ as that in the pure sample, indicating that a small amount of Zn-impurity does not affect the phonon thermal conduction. In contrast, the light Zn doping for the superconducting crystal strongly suppresses T_c down to 80K through the superconducting pair breaking, resulting in a reduced peak in $\kappa_{ab}(T)$ in Fig.1(a)[18].

We notice a common trend in the temperature dependence of phonon component between as-grown and superconducting samples. For example, $\kappa_{ab}(T)$ of both as-grown and oxygen-annealed samples with x=0 shows a weakly T^{-1}-like behavior at high-T. In addition, the oxygen content does not affect the T dependence of κ_{ph} strongly except for highly insulating crystal $YBa_2Cu_3O_{6+\delta}$($\delta \leq 0.11$) [19, 17]. Accordingly, let us assume that a minor modification of $\kappa_{ab}(T)$ of as-grown crystals expresses the temperature

variation of the phonon component below T_c for superconducting crystals if we ascribe the κ peak to the electronic contribution. Thus, the original κ data for as-grown crystals are scaled to coincide with $\kappa_{ab} - \kappa_e^n$ for the corresponding superconducting crystals at high temperatures (150K). The solid and dashed curves in Fig.1 represent the phonon contribution and , at the selected temperature of 40K, we obtain 43 % at $x = 0$, 55 % at $x = 0.1$ and 71 % at y(Zn)=0.0071. (the corresponding electronic component is listed in Table 1) This rough estimation in κ_{ph} is comparable with the value ($\sim$ 40% near $T_c/2$ for $YBa_2Cu_3O_{7-\delta}$ with $7 - \delta = 6.93$) evaluated by Takenaka et al., [17]. Separately, a primitive estimation on the phonon component of an untwinned crystal YBCO with T_c=90.5K gives a similar value [4].

Next, we show in the Fig.4 the magnetic field dependence of the in-plane thermal conductivity $\kappa_{ab}(H)$ of single crystals $(Y_{1-x},Sm_x)Ba_2Cu_3O_{7-\delta}$ (x=0, 0.1 and 1.0) and $YBa_2(Cu_{1-y}Zn_y)_3O_{7-\delta}$ (y=0.0071). The $\kappa_{ab}(H)$ data are normalized by the zero field value. At low fields, the value of κ_{ab} exhibits a rapid drop around nearly $T_c/2$ and it then tends to saturate at high fields up to 14 T. The applied field causes a substantial decrease in $\kappa(H)/\kappa(0)$ by $\sim$ 30% at x=0, while $\kappa(H)/\kappa(0)$ of Sm-substituted samples shows a smaller degradation from $\sim$ 16% at x=0.1 to $\sim$ 12% at x=1.0. In the mixed state of conventional superconductors, we believe that thermal carriers (quasiparticles and phonons) are scattered by the magnetic vortices, resulting in a substantial decrease in κ.

Now, we try to fit the $\kappa_{ab}(H)$ data to the electronic contribution model [8, 9]. The electronic thermal conductivity in magnetic fields, $\kappa_e(T, H)$, is rewritten using both $\kappa_e(T, 0)$and ℓ_0 as follows;

$$\kappa_e(T,H) = \frac{1}{3}C_e(T)v_f\ell(T,H) = \kappa_e(T,0)\frac{\ell(T,H)}{\ell_0(T)} = \frac{\kappa_e(T,0)}{1+\ell_0(T)/\ell_v(H)} \quad (1)$$

Here, the total mean free path of quasiparticles is expressed such as $\ell(T,H)^{-1} = \ell_0(T)^{-1} + \ell_v(H)^{-1}$, where ℓ_0 and ℓ_v are the mean free path of quasiparticles in zero field and in sufficiently strong fields, respectively.

Accordingly, the field dependence of the thermal conductivity ,$\kappa(T, H)$,is fitted using the following formula

$$\kappa(T,H) = \kappa_e(T,H) + \kappa_{ph}(T) = \frac{\kappa_e(T,0)}{1+p(T)H^n} + \kappa_{ph}(T) \quad (2)$$

,where we set $p(T)$ as $\sigma\ell_0/\phi_0$ and $\ell_0/k\sqrt{\phi_0}$, for n=1 and 0.5, respectively (ϕ_0, the quantum flux). In the case of $n = 1$, σ represents a scattering cross section per vortex cores in transport [20]. When the quasiparticle scattering from vortex cores is proportional to the number of the magnetic quantum flux, we get $\ell_v(H)^{-1}$=$\sigma H/\phi_0$[21]. Thus, for the exponent n=1 in eq. (2), we take into account for the mean free path of quasiparticles $\ell_v(H)$ from the scattering due to vortex cores, in addition to ℓ_0 for scattering processes in the Meissner state. Using the $\sigma = 90$ $\mathring{A}$ in YBCO [21], $\ell_v(H)$ is $\sim$ $2.3 \times 10^3 H^{-1}$ ÅT^{-1}. On the other hand, in the case of n=0.5, assuming the quasiparticle scattering due to screening currents around vortex cores in a disordered

vortex array, the vortex contribution $\ell_v(H)$ is proportional to the average lattice constant of a vortex lattice a_v i.e., $\ell_v(H) = ka_v \simeq k\sqrt{\phi_0/H}$, where k is a constant independent of fields [22]. Using k=0.5 in [22], $\ell_v(H)$ becomes $\sim 2.2 \times 10^2 H^{-1/2}$ ÅT$^{-1/2}$.

Our reliable fits of the $\kappa(H)$ data to Eq.(2) give the two parameters, $\kappa_e(T,0)/\kappa$(=1-κ_{ph}/κ) and $p(\propto \ell_0)$, at selected temperatures as summarized in Table 1. It is truly that our fitting procedures yield a better fit for the $n = 1$ than that for the $n = 0.5$, but it is difficult to distinguish a H-linear or $\sqrt{H}$-dependence in the denominator of $\kappa(H)$ in Fig.4. In H-linear fits, we notice the underestimation in electron component for all crystals if we accept the phonon component estimated from the as-grown data. For example, in the pure crystal of x=0, the H-linear fit yields $\kappa_e \sim 32\%$, while in the $\sqrt{H}$ fit we get $\kappa_e \sim 50\%$. This tendency in κ_e below T_c appears in previous works on the field dependences of $\kappa(H)$ for underdoped $YBa_2Cu_3O_{6.63}$ and $Tl_2Ba_2CuO_6$[8, 21]. Such the underestimation in κ_e will enable us to consider a significant modification of the free-electron Lorenz number in the WF law for the strongly electron correlated system such as high- T_c cuprates, giving the reduced electron thermal conductivity [23].

Finally, let us examine the fitting parameter p listed in Table1. From $p \propto \ell_0$, we obtain the mean free path of quasiparticles $\ell_0 \sim 1.1 \times 10^{-7}$m for n=1 at the pure crystal. Here, we used the cross section of $\sigma = 90$ $\mathring{A}$ in YBCO [21]. In a similar way, for the n=0.5, $\ell_0 \sim 7.8 \times 10^{-6}$m with k=0.5 in [22]. Both the former and latter fits give ℓ_0 ∼1000$\mathring{A}$ at 40K for pure x=0 crystal. From Table1, we guess that ℓ_0 at the Sm substituted crystal is about one-third as long as the value of ℓ_0 of the pure crystal, whether we use the H-linear fit or the $\sqrt{H}$. If the normal state $\kappa_e(T)$ is proportional to $\ell_0(T)$ at $T \geq T_c$, then the κ_e^n plots in Fig.3(a)give the ratio of ℓ_0 at x=0.1 to that at x=0 ~ 0.26 at higher T , This value is not far from the above results in the ℓ_0 ratio ($\sim 1/3$) around a half of T_c. Moreover, for the lightly Zn-doped crystal, our fits to the data indicate the reduced mean free path of quasiparticles. A pair-breaking effect due to Zn-doping makes quasiparticles increase, giving the strongly electron-electron scattering enhanced below T_c. This finding has a close relationship with the reduced peak observed in κ_{ab} of $YBa_2(Cu_{1-y}Zn_y)_3O_{7-\delta}$ with y=0.0071.

4. Summary

We have studied the in-plane thermal conductivity of large single crystals $(Y_{1-x},Sm_x)Ba_2Cu_3O_{7-\delta}$ (x=0, 0.1, 0.2 and 1.0) and $YBa_2(Cu_{1-y}Zn_y)_3O_{7-\delta}$ (y=0.0071) as functions of temperature and magnetic field. The nonlinear field profile of $\kappa(H)$ observed around a maximum peak is discussed on the basis of the electron contribution model. We tried to make the fits of the $\kappa(H)$ data to the H-linear or $\sqrt{H}$ dependence of the inverse electronic thermal conductivity in Eq.(2). The local distortion due to the Sm substitution for Y site suppresses both the phonon and electronic contributions, accompanied by the substantial decrease in ℓ_0 at 40K in comparison with that of the x=0 pure sample. The light Zn doping for CuO_2 planes does not contribute the phonon conduction but affects solely the electron component below T_c, resulting in the reduced

mean free path of quasiparticles in the superconducting state. For SmBCO, a suppressed maximum in $\kappa(T)$ arises from the partial substitution of Sm for Ba site ,which is closely related to the slight degradation in T_c.

One of authors (X Yao) would like to thank NBRPCE(No.2006CB601003) and SSTC (No.055207077) for financial support. We are grateful to F.Sato and Prof.S.Kambe for the iodometric analysis.

References

[1] C.Uher, J.Supercond.3,337(1990).
[2] J.M.Ziman,Electrons and Phonons. Clarendon Press, Oxford,1960.
[3] L.Tewordt and T.H.Wolkhausen, Solid State Commun.70,839(1989).
[4] R.C.Yu, M.B.Salamon, J.P.Lu, and W.C.Lee, Phys.Rev.Lett.69, 1431(1992).
[5] D.A.Bonn, Ruixing Liang,T.M.Riseman,et al.,Phys.Rev.B47,11314(1993).
[6] S.D.Peacor,J.L.Cohn,and C.Uher, Phys.Rev.B43,8721(1991).
[7] R.A.Richardson, S.D.Peacor,J.L.Cohn,F.Nori, and C.Uher, Phys.Rev.Lett. 67,3856(1991).
[8] F.Yu, M.B.Salamon, V.N.Kopylov ,N.N.Kolesnikov, H.M.Duan and A.M.Hermann, Physica C235-240, 1489(1994).
[9] Y.Pogorelov, M.A.Arranz,R.Villar, and S. Vieira, Phys.Rev.B51,15474(1995).
[10] S.T.Ting,P.Pernambuco-Wise, and J.E.Crow, Phys.Rev.B50,6375(1994).
[11] R.K.Williams,P.M.Martin,and J.O.Scarbrough,Phys.Rev.B59,13639(1999).
[12] X.Yao,M.Nakamura,M.Tagami,and Y.Shiohara, Physica C272,227(1996).
[13] K.Krishana,J.M.Harris,and N.P.Ong, Phys.Rev.Lett.75,3529(1995).
[14] X.Yao,T. Izumi, and Y.Shiohara, Supercond.Sci. Technol.16,L13(2003).
[15] X.Yao,K.Ohtsu,S.Tajima,H.Zama,F.Wang, and Y.Shiohara, J.Mater.Res.11,1120(1996).
[16] M.Matsukawa,T.Mizukoshi, K.Noto,and Y.Shiohara, Phys.Rev.B53,R6034(1996).
[17] K.Takenaka,Y.Fukuzumi,K.Mizuhashi, and S. Uchida, Phys.Rev.B56,5654 (1997).
[18] P.J.Hirschfeld and W.O.Putikka, Phys.Rev.Lett.77,3909(1996).
[19] J.L.Cohn,C.K.Lowe-Ma, and T.A.Vanderah,Phys.Rev.B52,R13134(1995).
[20] R.M.Cleary,Phys.Rev.175,587(1968).
[21] N.P.Ong, K. Krishana, Y. Zhang and Z.A.Xu, cond-mat/9904160.
[22] M.Franz, Phys.Rev.Lett.82, 1760(1999).
[23] Y.Zhang,N.P.Ong,Z.A.Xu,K.Krishana,R.Gagnon, and L.Taillefer, Phys.Rev.Lett.84, 2219(2000).

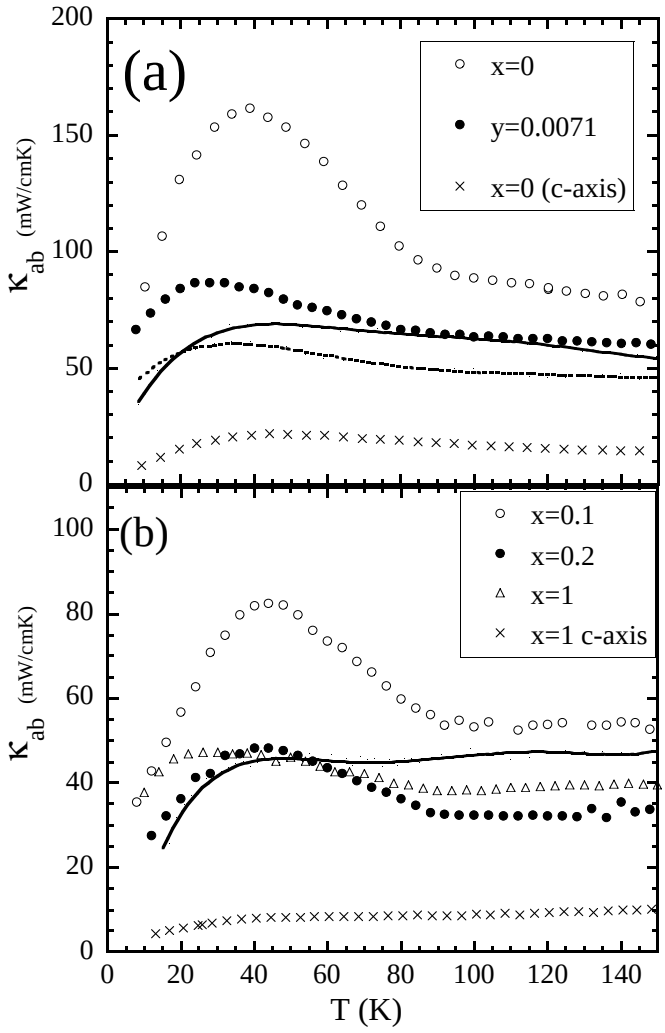

Figure 1. The in-plane thermal conductivity κ_{ab} for single crystals $(Y_{1-x},Sm_x)Ba_2Cu_3O_{7-\delta}$ (x=0, 0.1, 0.2 and 1.0) and $YBa_2(Cu_{1-y}Zn_y)_3O_{7-\delta}$ (y = 0.0071) as a function of temperature. For comparison, the out-of-plane thermal conductivity $\kappa_c$with x=0 and 1.0 is also depicted. Solid and dashed curves in (a) represent the estimated phonon component κ_{ph} for x=0 and y = 0.0071,respectively (see to the text). In a similar way, a solid curve in (b) shows the phonon contribution κ_{ph} of the x=0.1 crystal.

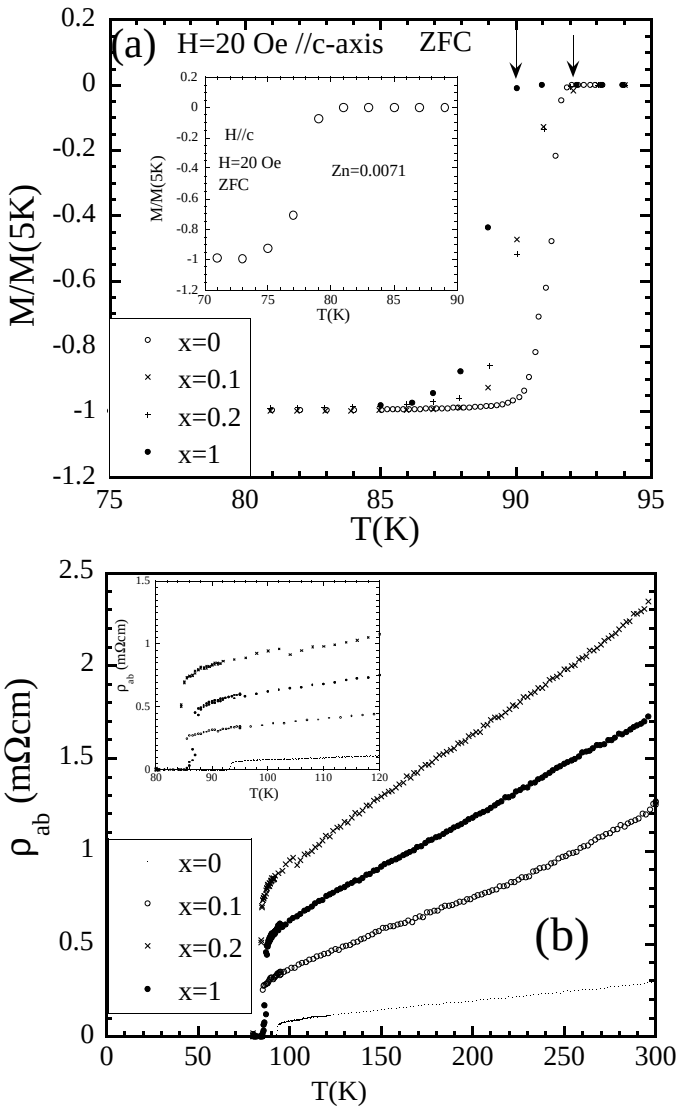

Figure 2. (a)normalized low-field magnetization $M(T)$ under a zero-field cooling (ZFC) scan and (b) in-plane resistivity $\rho_{ab}(T)$, for single crystals $(Y_{1-x},Sm_x)Ba_2Cu_3O_{7-\delta}$ (x=0, 0.1, 0.2 and 1.0). The $M(T)$ data of $YBa_2(Cu_{1-y}Zn_y)_3O_{7-\delta}$ (y = 0.0071) are given in the inset of (a). The inset of (b) represents magnified plots for the $\rho_{ab}(T)$ data of the Sm-substituted samples.

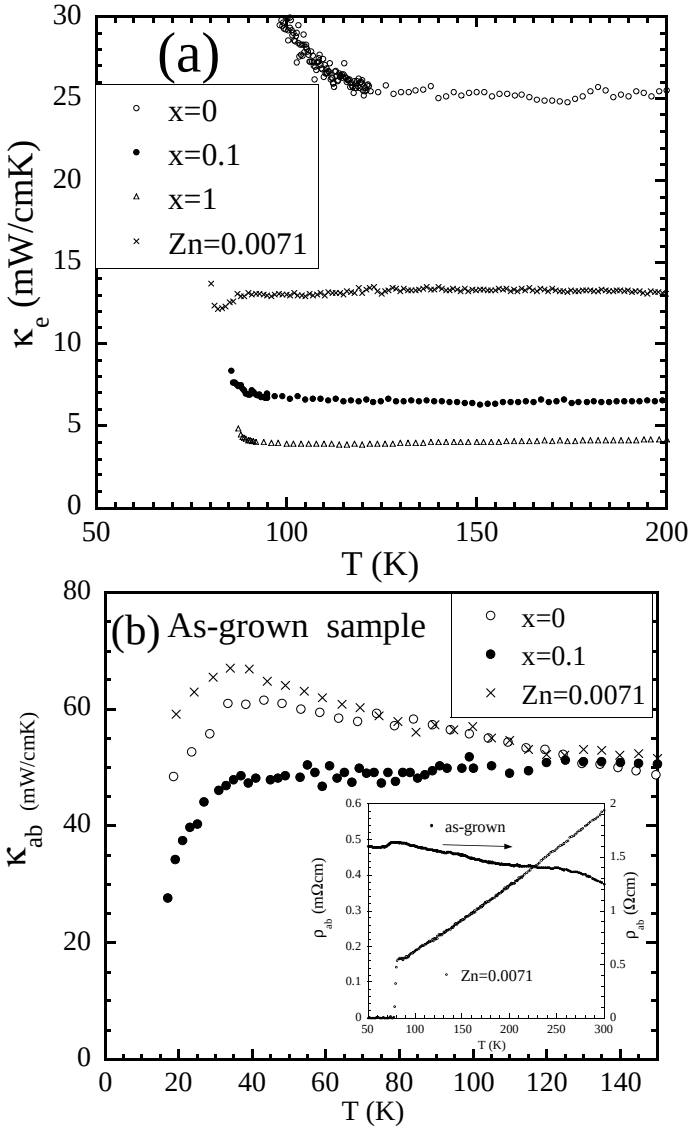

Figure 3. (a) Normal-state electronic thermal conductivity κ_e^n estimated from the resistivity data using the Wiedemann-Franz (WF) law $\kappa_e^n = L_0T/\rho$ with a Lorentz number L_0 =2.45×10^{-8}WΩ/K^2. (b) The κ_{ab} data for the corresponding as-grown crystals of $(Y_{1-x},Sm_x)Ba_2Cu_3O_{7-\delta}$ (x=0 and 0.1) and $YBa_2(Cu_{1-y}Zn_y)_3O_{7-\delta}$ (y=0.0071). In the inset of (b), the $\rho_{ab}(T)$ data for the as-grown and oxidized samples with light Zn doping are presented.

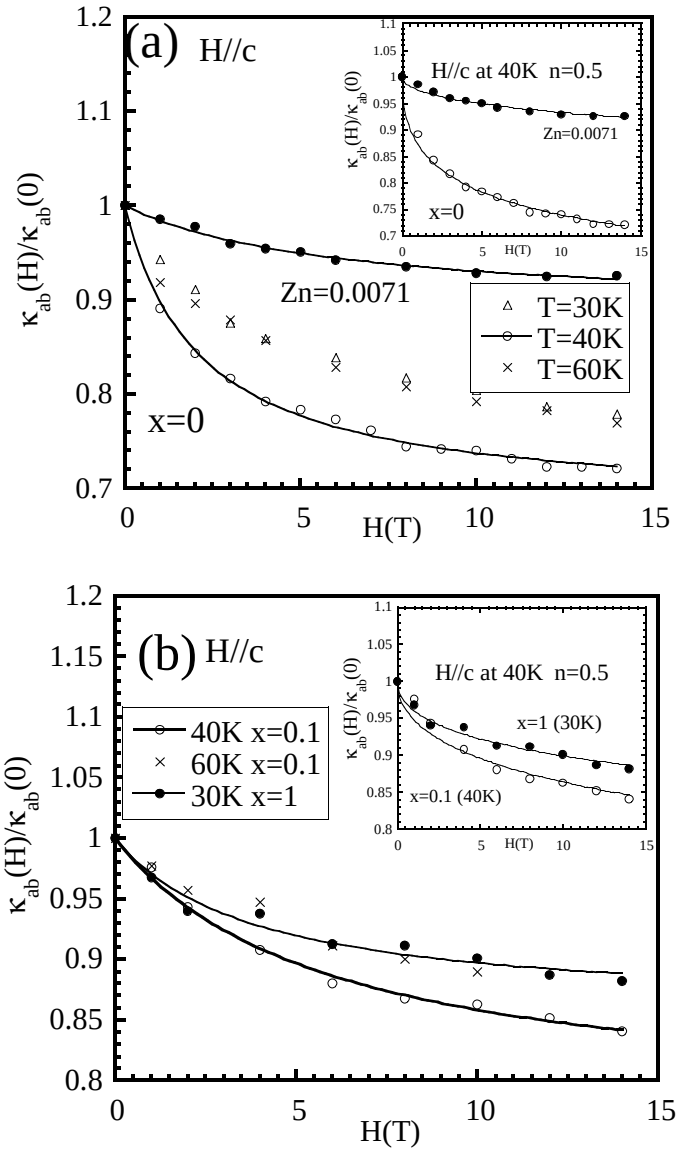

Figure 4. The magnetic field dependence of the in-plane thermal conductivity $\kappa_{ab}(H)$ of single crystals $(Y_{1-x},Sm_x)Ba_2Cu_3O_{7-\delta}$ (x=0, 0.1 and 1.0) and $YBa_2(Cu_{1-y}Zn_y)_3O_{7-\delta}$ (y=0.0071), at selected temperatures. The applied field H is parallel to the c-axis. Solid curves represent better fits of the $\kappa(H)$ data to the H-linear dependence of the inverse electronic thermal conductivity in Eq.(2). For comparison, the inset shows the curve fits to the $\sqrt{H}$-dependence of the inverse κ_e in Eq.(2).

Table 1. The fitting parameters κ_e/κ and p from the fit of $\kappa_{ab}(H)$ data to eq.(2)for single crystals $(Y_{1-x},Sm_x)Ba_2Cu_3O_{7-\delta}$ (x=0, 0.1 and 1.0) and $YBa_2(Cu_{1-y}Zn_y)_3O_{7-\delta}$ (y=0.0071). For comparison, we show the electronic component near $T_c/2$, estimated from the κ data of as-grown crystals described in the text. On the last column, the electronic components in the normal state are given using the WF law.

Sample		$n=1$			$n=0.5$			estimation	WF law
Composition	T	κ_e/κ	p	ℓ_0	κ_e/κ	p	ℓ_0	κ_e/κ	κ_e/κ(150K)
x	(K)	(%)		Å	(%)		Å	(%)	(%)
0.0	40	32	0.46	1.1×10^3	50	0.34	7.8×10^2	57	31
0.1	40	22	0.17	4.1×10^2	53	0.11	2.5×10^2	45	12
1.0	30	14	0.26	6.2×10^2	35	0.13	3.0×10^2		10
y=0.007	40	11	0.17	4.1×10^2	30	0.09	2.1×10^2	29	22